



INTERNATIONAL ATOMIC ENERGY AGENCY
UNITED NATIONS EDUCATIONAL, SCIENTIFIC AND CULTURAL ORGANIZATION
INTERNATIONAL CENTRE FOR THEORETICAL PHYSICS
I.C.T.P., P.O. BOX 586, 34100 TRIESTE, ITALY, CABLE: CENTRATOM TRIESTE



SMR.764 -1

RESEARCH WORKSHOP ON CONDENSED MATTER PHYSICS
13 JUNE - 19 AUGUST 1994

WORKING GROUP ON
"DISORDERED ALLOYS"
8 - 19 AUGUST 1994

"Order and Phase Stability in Alloys"

Francois DUCASTELLE
Office National d'Etudes et de Recherches Aerospatiales
29, Avenue de la Division Leclerc
B.P. 2, F-92322 Cedex
Chatillon (Hauts-de-Seine)
FRANCE

These are preliminary lecture notes, intended only for distribution to participants

MAIN BUILDING - STRADA COSTIERA, 11 - TEL. 22401 TELEFAX 224163 TELEX 460392 - ADRIATICO GUEST HOUSE - VIA GRIGNANO, 9 - TEL. 224241 TELEFAX 224531 TELEX 460449
MICROPROCESSOR LAB - VIA BERGAMINI, 31 - TEL. 224271 TELEFAX 224600 TELEX 460392 - GALLERIA GUEST HOUSE - VIA BERGAMINI, 7 - TEL. 22401 TELEFAX 2240310 TELEX 460392

Order and Phase Stability in Alloys

by F. Ducastelle

(Cohesion and Structure, Volume 3)

1991 xiv + 512 pages Price: US \$ 151.50 / Dfl. 295.00 ISBN 0-444-86973-5

The main purpose of this book is to describe the modern tools of solid state physics (in particular, electronic structure calculations and statistical thermodynamics) that enable us to understand ordering effects in alloys and to determine phase diagrams. This approach is used more to throw light on the most important physical mechanisms rather than to be able to make accurate predictions suitable for particular applications. On the other hand, more phenomenological, practically oriented approaches can expand the scope of these new theoretical insights.

A second purpose of the book is to show that materials science can provide wonderful and too often ignored examples to test and discuss the most fundamental physical theories. For example, many real alloys on a face centered cubic lattice are marvellous examples of the Ising model on this lattice with many different ordered structures, commensurate or not.

Contents: Preface.

1. Order and phase stability: an introduction.
 2. Order and disorder on a crystalline lattice: the Ising model.
 3. The ground state of the Ising model.
 4. Mean field approximations for the Ising model and their limitations.
 5. Phase diagrams and ordering in alloys.
 6. Electronic structure and the coherent potential approximation.
 7. Effective pair interactions.
- Author index. Subject index.

NORTH-HOLLAND

Elsevier Science Publishers
P.O. Box 103
1000 AC Amsterdam
The Netherlands

In the USA & Canada:
Elsevier Science Publishing Co., Inc.
P.O. Box 882, Madison Square Station
New York, NY 10159, USA



US \$ prices are valid only in the USA and Canada. In all other countries, the Dutch Guilder price is definitive. Customers in The Netherlands, please add 6% BTW. In New York State, applicable sales tax should be added. All prices are subject to change without prior notice.

404/B/482



OFFICE NATIONAL D'ETUDES ET DE RECHERCHES AEROSPATIALES

29, av.de la Division Leclerc. Châtillon (Hauts-de-Seine)
Téléphone: (1) 46 73 40 40 - Télécopie : (1) 46 73 41 41

Adresse postale : BP 72, F - 92322 CHATILLON CEDEX

ORDER AND PHASE STABILITY IN ALLOYS

ORDRE ET STABILITE DE PHASE DANS LES ALLIAGES

F. DUCASTELLE

Electron Theory in Alloy Design

Edited by D.G. Pettifor and A.H. Cottrell, Vol. 534, pp. 122-157

Ce document ne peut être vendu

N° Rubrique : 76-77

N° DED : 4279

TIRE A PART N° 1993 - 10

Order and Phase Stability in Alloys

FRANÇOIS DUCASTELLE

Office National d'Etudes et de Recherches
Aérospatiales (ONERA) BP 72
92322 Châtillon Cedex, France

5.1 INTRODUCTION

Due to the presence of interatomic interactions, any alloy should eventually order or phase separate at low temperature. This is observed in many systems. When the ordering interactions are strong, the alloy may remain ordered up to the melting point (Ni₃Al for instance). When they are very weak, the solid solution can be the only observable phase since at low temperature atomic diffusion is no longer efficient (Cu-Ni). In the intermediate regime we have a more interesting situation with one or several ordered phases at low temperature which disorder at a critical temperature before melting (Cu-Au, Pd-V, Ni-Fe, etc.). In the simplest case all phases are built on a fixed underlying lattice such as the fcc or bcc lattice, but more frequently, several structures are involved and many compounds display structures which are not observed in elemental metals (Laves phases, σ phases, Al₃ phases, etc.).

It is of great interest, both from a fundamental and a practical point of view, to understand what stabilizes a particular structure at a given concentration and temperature and then to predict the phase diagrams of alloys.

Until recently, most theories in this field were based on phenomenological models. The stability of several crystalline structures has been interpreted using geometrical arguments by looking for the most effective way of filling space with hard spheres of different radii. Size effects are also known to account for the limits of stability of solid solutions. Chemical or electronic parameters have also been used. One of the celebrated Hume-Rothery rules for instance relates the stability of several structures to definite values of the electronic ratio (number of valence electrons per atom). Finally various electronegativity scales have been introduced. As far as phase diagrams are concerned, most approaches have been based on phenomenological thermodynamic models using regular solution models or various improvements on them.

Recent research indicates that it is now possible to tackle these problems from

microscopic theories based on first principles. This confidence is based on the success of first principles electronic structure calculations concerning elemental metals as well as intermetallic compounds, and on the development of efficient thermodynamic tools. In fact 'ideal' methods starting from the Schrödinger equation and from general thermodynamics are generally not so useful when one is interested in a physical understanding of fairly complex systems, and it is still quite valuable to define intermediate models containing a few relevant parameters.

Many modern studies use an approach similar to that presented in this short review which can be summarised as follows. We start from electronic structure models based on various well defined approximation: the one-electron approximation based on the so-called local density approximation, the tight-binding approximation when necessary, etc. These approximations are now well controlled in the case of elemental metals or simple ordered compounds and provide total energies with a very good accuracy. The next step is to calculate the energy of any atomic configuration which obviously cannot be done exactly. At this stage it is shown that this energy can be obtained through a generalised perturbation expansion starting from the disordered state. The latter is described within the coherent potential approximation which is the simplest method that allows us to treat the scattering of electrons in strongly disordered systems, i.e. in systems where the atomic potentials strongly differ from one atom to the other.

At the end of this process, the electronic degrees of freedom are eliminated and we are left with the desired expression for the energy of any configuration as a function of pair and multiple interactions. In the case of a binary alloy we recover the celebrated Ising model or direct generalisations of it, were it not for the concentration dependence of the interactions which is completely unavoidable in the theory. The implications of this dependence can be considerable, in particular when studying phase diagrams (principally because of the common tangent rule), but they are still far from being well characterised, both experimentally and theoretically, and it is hoped that at least locally on the concentration axis the previous theory offers a good justification for the use of Ising models.

The next step is therefore a thermodynamic one and consists in exploring the properties of the Ising model, i.e. studying the nature and the stability of ordered structures as a function of concentration, temperature and of the interactions. Exact results can be obtained at zero temperature but approximations are required at finite temperature. In the case of short-range interactions the modern developments of generalised mean field methods such as the cluster variation method now provides very accurate results, as tested by Monte Carlo simulations.

We are thus able in principle to go from electronic structure calculations to phase diagrams through a set of well controlled approximations. At least this is so when ordering effects can be assumed to take place on a fixed, rigid lattice.

These restrictions are rather important, since they are necessary in order to speak of Ising models with discrete numbers of degrees of freedom per site. However even if this has still not been worked out in detail there is no difficulty in principle in extending the whole chain of arguments to include elastic and relaxation effects; it is also possible to compare ordered structures on different types of lattices, i.e. to treat structural effects.

The fact that such an approach can now be implemented is certainly an important result of recent years. It should be stressed however that the number of approximations introduced to derive in the end models with a few physical parameters, necessarily implies some loss of accuracy when studying concrete situations. Phenomenological models remain necessary to account in detail for experimental data, but on the other hand they cannot be reliable globally if they are not consistent with what is learned from more fundamental theories.

The present review is somewhat schematic. Details can be found in a recent book.¹ Several other important topics not discussed here can be found in the review by de Fontaine, in the books by Khachatryan and Hafner and in those of the series *Cohesion and Structure*.^{2,3,4,5}

Sections 5.2 to 5.5 are concerned with the electronic structure of alloys and with the derivation of effective multi-atom interactions. The thermodynamics of ordering effects is discussed in sections 5.6 and 5.7. Finally a few applications are presented in section 5.9.

5.2 TIGHT-BINDING MODEL FOR ALLOYS

The tight-binding formalism described in Chapter 4 is particularly well adapted to a semi-quantitative discussion of strong alloying effects. It also applies quite naturally to transition alloys. Furthermore there is no difficulty in principle, if not in practice, to derive the appropriate extensions involving full band structure calculations.

We consider here binary alloys $A_{1-x}B_x$ on fixed underlying lattices. For convenience we assume crystalline structure with a single atom per unit cell (e.g. fcc or bcc). Each atomic configuration is characterised by the value of the so-called occupation numbers p_n^i equal to unity or zero depending on the presence or not of an atom of type i at site n ; obviously $p_n^B = 1 - p_n^A$. The simplest tight-binding hamiltonian H can then be written in the Dirac notation (see Appendix) as

$$H = \sum_n |n\rangle \epsilon_n \langle n| + \sum_{n \neq m} |n\rangle \beta_{nm} \langle m| \quad (5.1)$$

where $|n\rangle$ is an atomic state centred on site n and ϵ_n, β_{nm} are the corresponding atomic level and hopping integrals, namely

$$\epsilon_n = \sum_{i=A,B} p_n^i \epsilon^i \quad (5.2a)$$

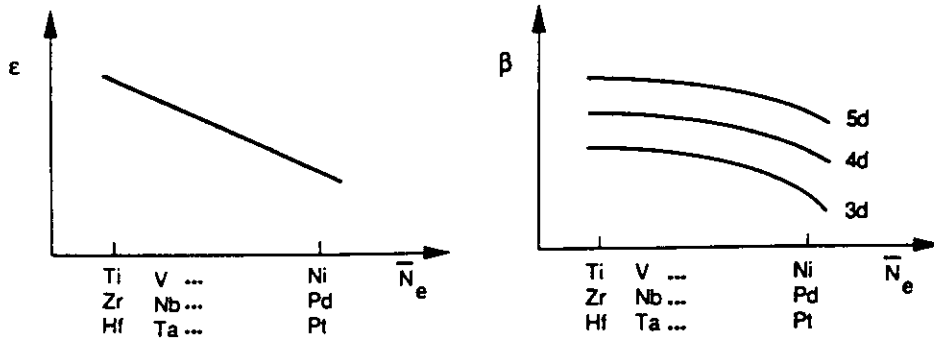


Fig. 5.1 Typical variations of the atomic levels and of the hopping integrals as a function of the mean number of electrons \bar{N}_e .

$$\beta_{nm} = \sum_{ij=A,B} \rho_n^i \rho_m^j \beta_{nm}^{ij} \quad (5.2b)$$

In the case of transition alloys the degeneracy of the d states has to be included, but for simplicity we shall drop here the corresponding indices which can easily be reintroduced when necessary. In this simple scheme, the electronic structure of the alloy is then characterised by a few parameters. Taking as the origin of energy the mean atomic level $\bar{\epsilon} = (1 - c)\epsilon^A + c\epsilon^B$, an important parameter is the so-called diagonal disorder parameter $\delta = \epsilon^B - \epsilon^A$ which plays the part of an electronegativity difference. The off-diagonal disorder is then related to the differences between the hopping integrals. A very convenient and reasonable approximation is to set $(\beta^{AB})^2 \approx \beta^{AA} \cdot \beta^{BB}$. Since the widths W^A and W^B of the pure elements are proportional to β^{AA} and β^{BB} respectively, off-diagonal disorder can be characterised by the ratio $(W^A - W^B)/\bar{W}$ where \bar{W} is the mean band width. The bandwidth of transition metals decreases along a transition series and increases from the 3d to the 5d series with extreme values of the order of 4 and 8 eV. The energy levels on the other hand decrease about one eV per element (see Fig. 5.1).

In many cases then, off-diagonal disorder can be neglected (a typical exception would be Zr-Ni alloys) and the principal parameter is the dimensionless ratio δ/\bar{W} which is at most of the order of unity for alloy constituents with very different number of d electrons N_e^A and N_e^B . When $\delta/\bar{W} \ll 1$ standard perturbation theory applies, and to lowest order the density of states is that of an effective metal of bandwidth \bar{W} and centred on the mean level $\bar{\epsilon}$. From very general arguments it is then easy to determine the qualitative shape of the density of states as a function of the degree of order and of the concentration (Fig. 5.2).

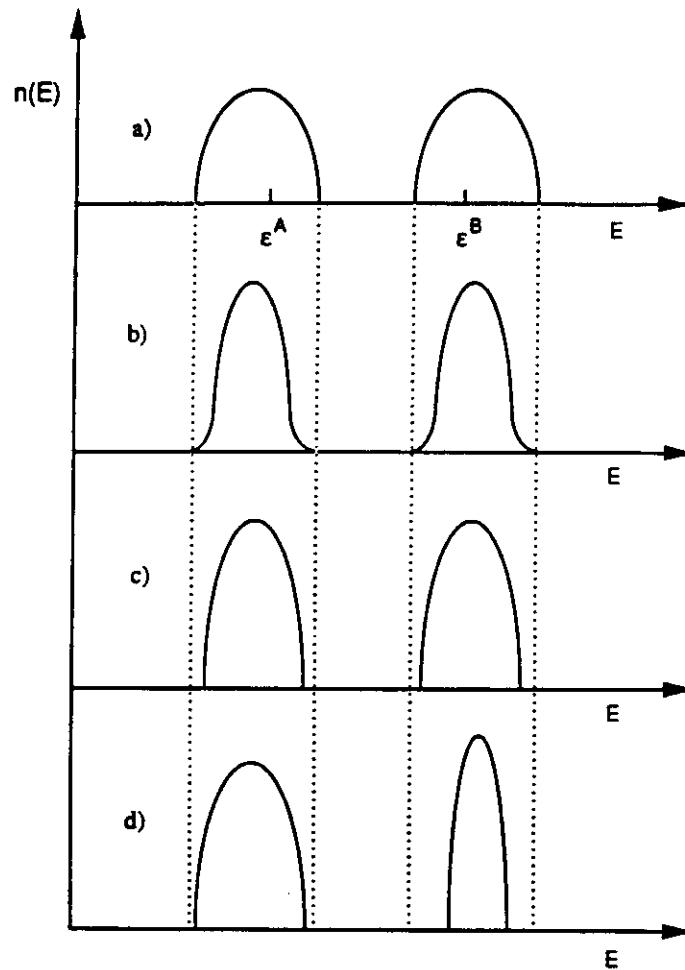


Fig. 5.2 Schematic densities of states: (a) for a two-phase alloy, (b) for a disordered alloy, (c) for an ordered alloy. In all cases $c = 1/2$. The density of states for an alloy when $c > 1/2$ is shown in (d).

5.3 ELECTRONIC STRUCTURE OF DISORDERED ALLOYS

We want to calculate the density of states of a completely disordered alloy, i.e. such that the occupations of different sites are completely uncorrelated. Using ensemble averages $\langle \dots \rangle$ over all possible atomic configurations for a given concentration, this means that

$$\begin{aligned} \langle p_n \rangle &= c \\ \langle p_n p_m \rangle &= c^2 \text{ if } n \neq m \end{aligned} \tag{5.3}$$

✱

$$= c \text{ if } n = m$$

where we have set $p_n \equiv p_n^B$. It is not possible to calculate exactly the average density of states $\langle n(E) \rangle$. Some formalism is necessary to see where are the difficulties. Following the Appendix on Green functions, we start from the formula

$$n(E) = \text{Tr} \delta(E - H) = \lim_{\epsilon \rightarrow 0} - \frac{\text{Im}}{\pi} \text{Tr} G(E + i\epsilon) \quad (5.4)$$

where Tr denotes the trace over the states $|n\rangle$, Im the imaginary part and G the so-called resolvent or Green function

$$G(z) = (z - H)^{-1} \quad (5.5)$$

where z is a complex number. Assuming diagonal disorder only, H can be split into two parts

$$H = H^0 + V$$

with

$$H^0 = \sum_{n,m} |n\rangle \beta_{nm} \langle m| \quad (5.6)$$

$$V = \sum_n |n\rangle \epsilon_n \langle n|$$

where H^0 does not depend on the atomic configuration. Defining the bare Green function G^0 through $G^0 = (z - H^0)^{-1}$, we write the *Dyson equation* for G

$$\begin{aligned} G &= G^0 + G^0 V G \\ &= G^0 + G^0 V G^0 + G^0 V G^0 V G^0 + \dots \end{aligned} \quad (5.7)$$

One should of course be careful in this kind of calculation not to forget the non-commutativity of operators. Consider now the average of the second order term

$$\langle G^0 V G^0 V G^0 \rangle = G^0 \langle V G^0 V \rangle G^0 \quad (5.8)$$

and take its matrix element; we have

$$\langle (V G^0 V)_{mm} \rangle = \sum_{i,j} \langle p_n^i p_m^j \rangle \epsilon^i \epsilon^j G_{nm}^0 \quad (5.9)$$

so that, according to equation (5.3) $\langle VG^0V \rangle$ does not reduce to $\langle V \rangle G^0 \langle V \rangle$. We have instead

$$\langle VG^0V \rangle - \langle V \rangle G^0 \langle V \rangle = \sum_{\mathbf{n}} |n\rangle c(1-c)\delta^2 G_{\mathbf{n}}^0 \langle n| \quad (5.10)$$

It is then useful to define an effective potential $\Sigma(z)$ through

$$\langle G \rangle = G^0 + G^0 \Sigma \langle G \rangle = (z - H^0 - \Sigma(z))^{-1} \quad (5.11)$$

$\Sigma(z)$ is a complex operator which can be expanded in successive powers of δ

$$\Sigma(z) = \sum_{\mathbf{n}} |n\rangle c(1-c)\delta^2 F^0(z) \langle n| + \dots \quad (5.12)$$

where $F^0(z) = G_{\mathbf{n}}^0$ is the diagonal matrix element of G^0 .

It is impossible to sum exactly this series, but we want at least to go beyond second order in δ . Different methods can be used. The simplest approximation is the so-called coherent potential approximation (CPA) which is a mean field theory determining the best possible local effective potential, i.e. such that

$$\Sigma(z) \approx \sum_{\mathbf{n}} |n\rangle \sigma(z) \langle n| \quad (5.13)$$

The subject is well documented and we skip here the details which can be found in previous reviews.^{1,6} Defining the local t -matrix t^i

$$t^i = (\epsilon^i - \sigma)[1 - (\epsilon^i - \sigma)F]^{-1} \quad (5.14)$$

where $F(z) = F^0(z - \sigma(z))$, the self-consistent CPA equation for $\sigma(z)$ is

$$\langle t \rangle = ct^B + (1-c)t^A = 0 \quad (5.15)$$

When the CPA equation is solved the average density of states per site is simply given by

$$\langle n(E) \rangle = -\frac{\text{Im}}{\pi} F(E + i\epsilon) \quad (5.16)$$

Furthermore we also obtained local conditional density of states $n^i(E)$, i.e. the densities of states at a given site averaged over all configurations where the occupation $i = A, B$ of this site is held fixed

$$n^i(E) = -\frac{\text{Im}}{\pi} \{F[1 - (\epsilon^i - \sigma)F]^{-1}\} \quad (5.17)$$

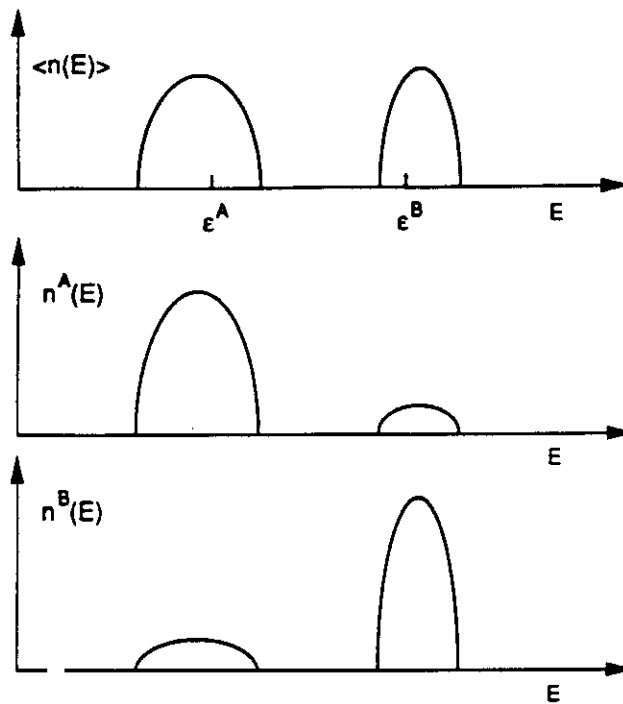


Fig. 5.3 Total and partial densities of states.

As expected the total density of states varies as shown in Fig. 5.2; schematic variations of the conditional densities of states are indicated in Fig. 5.3.

Local charges are obtained by integrating the conditional densities of states up to the Fermi level. In general we therefore obtain charge transfers. At this point some self-consistency rule is necessary since for example the diagonal disorder parameter δ has been considered up to now as an atomic quantity. The simplest rule, similar to that used for the pure elements and binary components (see section 4.4), is to postulate local neutrality. This implies that δ has to be self-consistently recalculated. In general, this yields values smaller than those deduced from the free atom energy levels; this is a typical feed-back effect.¹ Notice that global neutrality is always insured, by definition, since it is used to locate the Fermi energy.

5.4 ENERGY AND GENERALISED PERTURBATION EXPANSION

Exactly as in the case of pure metals the total energy of an alloy is directly related to its band energy when local neutrality is preserved. We therefore want

to calculate

$$U = \int^{E_F} dE E n(E) \quad (5.18)$$

where E_F is the Fermi energy. Since this energy is the electronic chemical potential at zero temperature, it is much more convenient to work with the grand potential $\Omega = U - E_F \bar{N}_e$, \bar{N}_e being the number of electrons, equal to $N(E_F)$ where $N(E)$ is given by

$$\begin{aligned} N(E) &= \int^{E_F} dE n(E) \\ &= \frac{\text{Im}}{\pi} \text{Tr} \log G(E + i\varepsilon) \end{aligned} \quad (5.19)$$

A straightforward integration by parts shows that

$$\Omega = - \int^{E_F} dE N(E) \quad (5.20)$$

All these formulae apply to any configuration of the alloy. We now compare the grand potential Ω with that of the disordered state calculated within the CPA. To this end we start from the Dyson equation (5.11) where $\langle G \rangle$ is replaced by its CPA value denoted \bar{G} . We then deduce that

$$\text{Tr} \log G = \text{Tr} \log \bar{G} - \text{Tr} \log [1 - (V - \Sigma)\bar{G}] \quad (5.21)$$

and finally

$$\begin{aligned} \text{Tr} \log G &= \text{Tr} \log \bar{G} - \sum_n \log [1 - (\varepsilon_n - \sigma)F] \\ &\quad - \text{Tr} \log [1 - i\hat{G}_{\text{off}}] \end{aligned} \quad (5.22)$$

where \hat{G}_{off} is the off-diagonal part of \bar{G} and \hat{t} is given by

$$\hat{t} = \sum_n |n\rangle t_n \langle n|; t_n = \sum_i p_n^i t^i \quad (5.23)$$

The term in the r.h.s. of equation (5.22) can be expanded as follows

$$- \text{Tr} \log [1 - i\hat{G}_{\text{off}}] = \frac{1}{2} \sum_{n \neq m} t_n \bar{G}_{nm} t_m \bar{G}_{mn} + \dots \quad (5.24)$$

Because $n \neq m$ the average of $t_n t_m$ in the completely disordered state reduces to

∧∧

the product of averages $\langle t_n \rangle \langle t_m \rangle$ which vanishes within the CPA. In fact, in the spirit of this approximation all other terms of the expansion can be neglected, and we deduce that the CPA average of $\text{Tr} \log G$ should be given by

$$\langle \text{Tr} \log G \rangle_{\text{CPA}} = \text{Tr} \log \bar{G} - \left\langle \sum_n \log [1 - (\epsilon_n - \sigma)F] \right\rangle \quad (5.25)$$

This can be verified by differentiating this expression with respect to z and is related to a very important property of the CPA.⁶

In the case of lattices with a single atom per unit cell, the second term in the r.h.s. of equation (5.22) is in fact independent of the atomic configuration for a fixed concentration and we finally obtain

$$\begin{aligned} \Omega &= \langle \Omega \rangle_{\text{CPA}} + \frac{\text{Im}}{\pi} \int^{E_f} \text{Tr} \log [1 - i\bar{G}_{\text{off}}] \\ &= \langle \Omega \rangle_{\text{CPA}} + \frac{1}{2} \sum_{n \neq m} \rho_n^i \rho_m^j V_{nm}^{ij} + \dots \end{aligned} \quad (5.26)$$

with

$$V_{nm}^{ij} = - \frac{\text{Im}}{\pi} \int^{E_f} dE t^i t^j \bar{G}_{nm}^2 \quad (5.27)$$

For a binary alloy, this can be written

$$\Omega = \langle \Omega \rangle_{\text{CPA}} + \frac{1}{2} \sum_{n \neq m} (\rho_n - c)(\rho_m - c) V_{nm} + \dots \quad (5.28)$$

$$V_{nm} = V_{nn}^{AA} + V_{mm}^{BB} - 2V_{nm}^{AB} = - \frac{\text{Im}}{\pi} \int^{E_f} dE (t^A - t^B)^2 \bar{G}_{nm}^2$$

This is the basic result of the previous, somewhat lengthy, calculations. Evidently such an expansion only makes sense if it is convergent. That this is generally true is explained in detail elsewhere.¹⁶ It turns out that the small parameter of the expansion is formally the product $i\bar{G}_{\text{off}}$ characterized by its matrix elements $t^i \bar{G}_{nm}$, $n \neq m$. Notice that when $\delta \rightarrow 0$, $t^B - t^A \approx \delta$ so that V_{nm} is of the order of δ^2/\bar{W} , in agreement with standard perturbation theory. Now t^i remains bounded when δ increases so that $t^i \bar{G}_{nm}$ can remain small. In fact this quantity depends on the energy and is not small by itself: it is only its contribution to integrals over the energy which is small. In other words, the generalised perturbation scheme described here is valid for energies, *not for densities of states*. Notice also that to lowest order, variations of grand potentials at constant

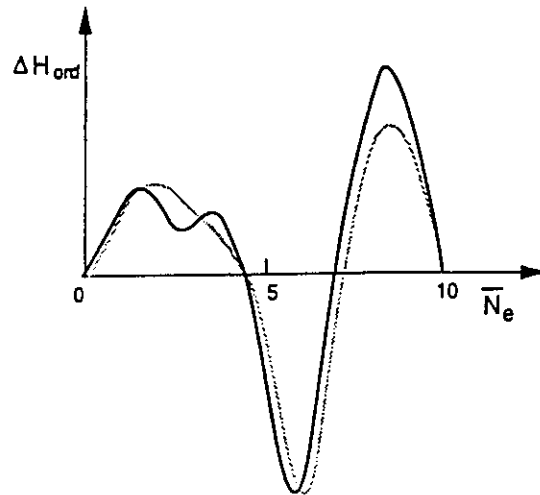


Fig. 5.4 Ordering energy for the DO_{22} structure for $\delta/\bar{W} = 0.45$. The full line corresponds to a recursion calculation whereas the dashed line corresponds to a calculation using effective pair interactions up to fourth nearest neighbours; after Bieber *et al.*⁷

Fermi energy are equal to variations of energy at fixed electronic concentration so that $\Omega - \langle \Omega \rangle_{\text{CPA}}$ is actually an ordering energy or enthalpy ΔH_{ord} .

To test the convergence of this generalised perturbation method (GPM) one can compare the ordering energy ΔH_{ord} of a given structure obtained from this development with that provided by a full electronic structure calculation, using recursion techniques for instance. Figure 5.4 shows the result of a calculation performed for the DO_{22} structure of a transition alloy on fcc lattice.⁷ In such a case one should of course reintroduce everywhere degeneracy indices. The comparison is indeed fairly satisfactory and furthermore it can be verified that it is even sufficient, on the scale of the figure, to keep only first neighbour interactions V_1 . This has been observed in many other cases. In fact the shape of the curve $\Delta H_{\text{ord}}(\bar{N}_e)$ is completely determined by that of $V_1(\bar{N}_e)$ which itself should necessarily display two zeros at least. This can be proved using moment arguments (see section 5.5).

It can be concluded that the generalised perturbation method (GPM) is rapidly convergent, except of course when the band filling is close to a zero of ΔH_{ord} . In such a case the *relative* error between the exact calculation and an approximate one can be important (see Fig. 5.4), and multi-atom interactions are relevant. It can be shown also that the convergence of the expansion also measures the validity of the CPA itself, so that conversely this convergence is not very good when the CPA is known to be inaccurate, as for example in the minority band; this is illustrated in Fig. 5.4, which shows that the convergence of the GPM is much better in the majority band (low values of \bar{N}_e) than in the minority band (high values of \bar{N}_e).

Imagine now that we have performed a genuine perturbation expansion as a function of δ/\bar{W} . Other pair V_{nm}^0 (and multi-atom) interactions would then be defined, different from the previous ones, but the development would be much less convergent, or not convergent at all. In other words, the choice of a 'good' medium of reference such as that provided by the CPA replaces a badly convergent expansion by a rapidly convergent one, the price to pay being the concentration dependence of the interactions through the concentration dependence of the self-energy σ . It is clear that this dependence is a simple way to account for complicated interactions in an average fashion. Note here that the interactions depend on the concentration for two reasons; the first has just been mentioned and the second is that the number of electrons \bar{N}_e , and therefore the electronic chemical potential, obviously vary with concentration. Contrary to the first, this other source of concentration dependence *does not disappear* when $\delta \rightarrow 0$. From a formal point of view, it is frequently useful to consider \bar{N}_e and c as independent variables. Then V_{nm} depends on c and on \bar{N}_e , whereas V_{nm}^0 only depends on \bar{N}_e .

The previous discussion shows that pair and multi-atom interactions do not have a real intrinsic nature. One can imagine that different media of reference can provide expansions with similar convergence properties. For a given configuration, different sets of interactions can yield similar energies, but one of course looks for a minimal set. What is argued here is that the generalised perturbation method naturally provides such a minimal set. In particular the hierarchy between the different relevant interactions is determined from the electronic structure and not assumed a priori.

This is to be contrasted with another frequently used method which may be called an inverse method. The idea is that if the ordering energy is considered as a (linear) function of a finite set of interactions, then these interactions can be determined from the calculation of the ordering energies of a sufficiently large number of ordered structures. Since this can be achieved with a very high accuracy, using first principles band structure calculations, it is sometimes argued that this is *the* way to proceed. There are however clear disadvantages with this approach; first the relevant interactions are at best determined using trial and error methods, but above all the physical interpretation of the variations of the interactions with various electronic parameters can be completely lost. In particular the fact that a minimum set of interactions should be concentration dependent is frequently overlooked in such methods.

Inverse and direct methods have been compared in detail by Sluiter and Turchi;⁸ see also Ferreira *et al.*,⁹ Wei *et al.*¹⁰ A comparison with different but similar perturbation expansions is also given in Gonis *et al.*¹¹ It is also possible to replace the CPA by numerical averages over configurations.¹² The concentration dependence of the interactions has also been discussed in this framework.¹³ Many results of these theories are very similar, which is quite easy to understand using the general arguments presented below.

To summarise: the generalised perturbation method (GPM) allows us to

Fig. 5.5 Path contributing to $\Delta\mu_4$.

describe ordering energies as a rapidly convergent sum of pair and multiatom interactions. The chain of arguments leading to this expansion is in fact quite similar to that used in pseudopotential theory. In both cases an appropriate choice of the medium of reference insures convergence of perturbation theory and second order terms always yield pair interactions. Note that the theory only describes ordering effects on a fixed lattice, and that it *does not assume* that the total energy of the crystal can be analysed in terms of pair interactions. As a matter of fact such a decomposition does not hold for the total energy of pure transition metals.

We have used the tight-binding scheme, but nothing prevents us writing similar equations using first principles formalism such as the KKR-CPA one (the correspondence between both formalisms is discussed elsewhere).^{1,6} In this sense the theory can be quasi-exact. Some calculations have already been performed in this direction.¹⁴

5.5 EFFECTIVE CLUSTER INTERACTIONS: TRENDS AND HIERARCHY

The generalised perturbation method generates effective pair and cluster interactions whose characteristics can be deduced from a simple moment analysis similar to that used for pure metals (see section 4.4.3). The normalised n^{th} moment of the density of states μ_n is given by

$$\mu_n = \frac{1}{N_s} \text{Tr} H^n \quad (5.29)$$

where N_s is the number of atoms. Using the decomposition $H = H^0 + V$, it is straightforward to realise that the first moment that depends on the atomic configuration at fixed concentration is the fourth one, the part depending explicitly on this configuration $\Delta\mu_4$ being proportional to $\text{Tr} H^0 V H^0 V$. Associating as usual with μ_n closed circuits of n elementary steps, we have here two types of steps: those involving the diagonal matrix elements represented by closed loops and those involving the hopping integrals associated with interatomic jumps (Fig. 5.5). This yields

$$\Delta\mu_4 = \frac{2}{N_s} \sum_{n,m} (p_n - c)(p_m - c) \beta_{nm}^2 \delta^2 \quad (5.30)$$

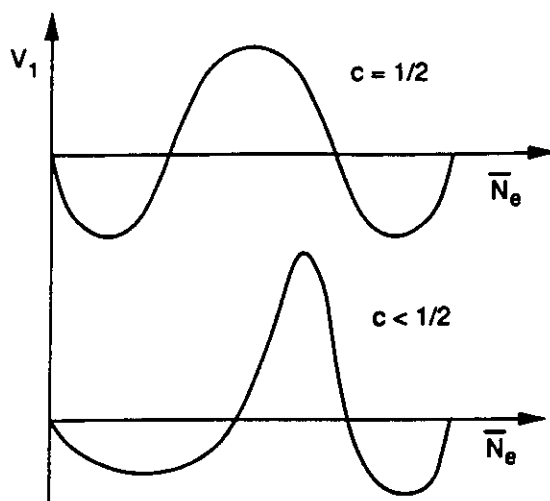


Fig. 5.6 Typical variations of $V_1(\bar{N}_e)$.

It can be shown on the other hand that the moments Δm_n of the ordering energy considered as a function of the Fermi energy are proportional to $-\Delta\mu_{n+2}$. Thus $\Delta m_0 = \Delta m_1 = 0$, $\Delta m_2 < 0$. More precisely, one can define moments of the pair and cluster interactions and equation (5.30) tells us that the second moment of the pair interaction V_{nm} is proportional to $-\beta_{nm}^2 \delta^2$. In general we only keep hopping integrals connecting an atom and those of its first coordination shell (first neighbours in the fcc lattice, first and second neighbours in the bcc lattice) so that only first neighbour (in this sense) pair interactions V_1 contribute to Δm_2 . The values of the first moments of $V_1(E_F)$ provide us with very useful sum rules from which we deduce that $V_1(\bar{N}_e)$ has in general two zeros and varies as indicated in the upper curve of Fig. 5.6. This shows that ordering (phase separation) is favoured for intermediate (extreme) fillings of the d band. Considering higher order moments it can be realised that the most important contribution to the third moment of V_1 is equal to $-(1 - 2c)\beta_{nm}^2 \delta^3$ which induces the asymmetry sketched in this figure.

Considering now further pair interactions, it is clear that they involve higher order moments. For example, in the fcc lattice we have a second class of neighbours, from the second to the fourth one, which can be reached in two steps (Fig. 5.7). Their first non-vanishing moment, related to $\Delta\mu_6$ is the fourth one. We therefore expect $V_{2,3,4}$ to be of the same order of magnitude. To be more precise one has to calculate the number of circuits involving a given pair, and also to take into account the fact that straight self-retracing paths contribute more than open ones.^{1,6} These effects have a tendency to cancel each other so that we predict the hierarchy $|V_1| \gg |V_2, V_3, V_4| \gg |V_5, \dots|$. This hierarchy is well observed in the numerical CPA calculations (Fig. 5.8). Similar arguments allow us to guess the hierarchy involving higher order cluster interactions. Once

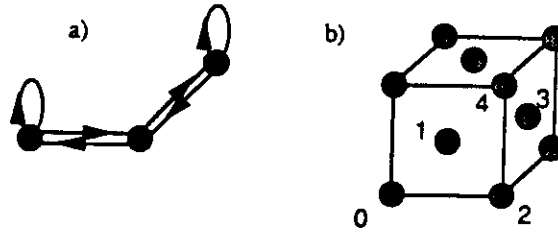


Fig. 5.7 (a) A path contributing to $\Delta\mu_6$ and therefore to M_4 . b) Nearest neighbour positions on the fcc lattice.

again the most important contributions are associated with straight paths. For example the most important triplet in a fcc lattice is that involving the first and fourth neighbours and may not always be negligible, compared to the pair interactions $V_{2,3,4}$.^{11,13,16}

Finally let us point out that several effects neglected up to now, but which can be very important when studying specific systems (such as the dependence on the crystalline structure, off-diagonal disorder, self-consistency, magnetism, etc.) can be discussed within the same scheme.^{1,6}

5.6 THERMODYNAMICS OF ALLOYS; LONG RANGE AND SHORT RANGE ORDER

We first recall the different notations used to describe the various configurations C of an alloy. Although these notations can be generalised to s -component alloys, we shall consider here binary alloys. As before we have in mind simple incompressible lattices with a single atom per unit cell. Any configuration is then specified by the set of values of the occupation numbers

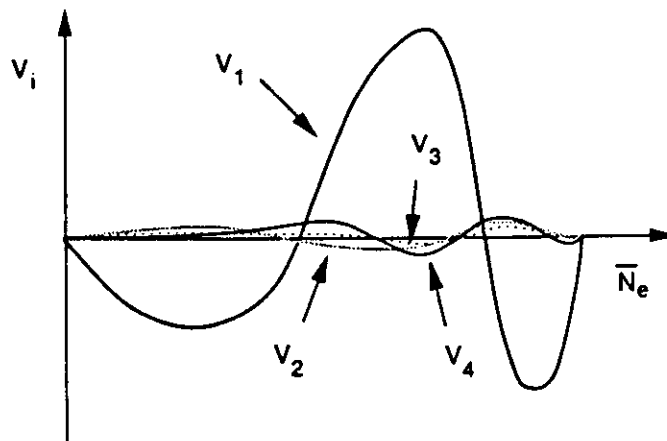


Fig. 5.8 Pair interactions on the fcc lattice; ($\epsilon = 1/4$, $\delta/\sqrt{V} = 0.45$); after Bieber.¹⁵

$p_n = p_n^B = 1 - p_n^A$. It is often more convenient to use a symmetrical notation and define spin-like variables $p_n = (1 + \sigma_n)/2$ so that σ_n takes on the value +1 or -1 depending on whether site n is occupied by an atom of type B or A. We have the obvious identities

$$p_n^2 = p_n; \sigma_n^2 = \sigma_n \quad (5.31)$$

Since we assume that each lattice site is occupied either by an A or by a B atom, the total number of B atoms is given by

$$N^B = \sum_n p_n = N_s c \quad (5.32)$$

where N_s is the number of atoms and c the concentration in B atoms.

At fixed volume, the relevant thermodynamic variables are the concentration c and the temperature T . The corresponding free energy $F(c, T)$ is given by

$$F = -k_B T \log \mathcal{Z} \quad (5.33)$$

with

$$\mathcal{Z} = \sum_C \exp [-E(C)/k_B T]$$

where $E(C)$ is the energy of the configuration C , k_B is the Boltzmann constant and the sum defining the partition function \mathcal{Z} is over all configurations of concentration c (canonical ensemble). It is useful at this point to compare this formalism with the more general one introduced in standard textbooks.¹⁷ The independent variables (at constant volume) are then the temperature and the numbers of atoms N^i of species i , and the corresponding free energy $F(N^i, T)$ satisfies

$$dF = -S dT + \sum_i \mu^i dN^i \quad (5.34)$$

$$F = \sum_i \mu^i N^i$$

where S is the entropy and $\mu^i(N^i, T)$ is the chemical potential of species i . In our case $N^A + N^B = N_s$ is constant and

$$dF = -S dT + (\mu^B - \mu^A) N_s dc \quad (5.35)$$

$$F = N_s \mu^A + (\mu^B - \mu^A) N_s c$$

In practice it is not easy to calculate sums over configurations at fixed con-

centration. The usual trick to lift this restriction is to take as independent variables T and the chemical potential difference $\Delta\mu = (\mu^B - \mu^A)$. We then replace $E(c)$ by $\tilde{E} = E - \Delta\mu N_s c$ and $F(c, T)$ by $\tilde{F}(\Delta\mu, T) = F - \Delta\mu N_s c$ so that

$$\tilde{F} = -k_B T \log \tilde{\zeta} \quad (5.36)$$

with

$$\tilde{\zeta} = \sum_{\mathbf{C}} \exp [-\tilde{E}(\mathbf{C})/k_B T]$$

where now the sum is over all atomic configurations (grand-canonical ensemble). Both formulations are equivalent in the thermodynamic limit $N_s \rightarrow \infty$. We have of course

$$d\tilde{F} = -S dT - N_s c d\Delta\mu \quad (5.37)$$

Within this formalism, the usual equilibrium conditions $\mu_\alpha^i = \mu_\beta^i$ when phases α and β coexist is replaced by conditions $\tilde{F}_\alpha = \tilde{F}_\beta$, $\Delta\mu_\alpha = \Delta\mu_\beta$.

In order to handle more symmetrical expressions we can again change slightly the notation by using as an independent variable in the canonical case the mean 'magnetisation' $m = 1/N_s \sum \sigma_s = 2c - 1$ rather than the concentration. Then equation (5.35) becomes

$$dF = -S dT + (\Delta\mu/2) N_s dm \quad (5.38)$$

$$F = N_s \frac{\mu^A + \mu^B}{2} + N_s m \Delta\mu/2$$

In a magnetic analogy, it is clear that $\Delta\mu/2$ plays the role of a magnetic field h . As usual then, equilibrium between two phases occurs at a fixed field h when $\tilde{F}_\alpha(h, T) = \tilde{F}_\beta(h, T)$ where here $\tilde{F} = F - N_s m h$ so that

$$d\tilde{F} = -S dT - N_s m dh \quad (5.39)$$

It will be clear in the following in which ensemble we are working and what are the considered variables, so that free energies and other related quantities will only be distinguished by their arguments (c, T) , $(\Delta\mu, T)$ or (h, T) .

To handle non-homogeneous systems it is finally useful to introduce site-dependent fields h_s . The corresponding free energy $F(\{h_s\}, T)$ is then given by

$$F(\{h_s\}, T) = -k_B T T r \log \exp[-H(\{\sigma_s\})]/k_B T \quad (5.40a)$$

where

$$H(\{\sigma_s\}) = E(\{\sigma_s\}) - \sum_s h_s \sigma_s \quad (5.40b)$$

is the 'energy' considered as function of the spin variables σ_n and the notation Tr , for trace means that we sum over all configurations, i.e. over all values ± 1 of these spin variables. H should not be confused with the electronic Hamiltonian used in the previous sections.

The thermodynamic average $\langle Q \rangle$ of any quantity Q can now be written

$$\langle Q \rangle = \frac{1}{\mathcal{Z}} \sum_{\mathbf{C}} \exp[-E(\mathbf{C})/k_B T] = Tr \rho(\{\sigma_n\}) Q(\{\sigma_n\}) \quad (5.41a)$$

with

$$\rho = \frac{1}{\mathcal{Z}} \exp[-H(\{\sigma_n\})/k_B T] \quad (5.41b)$$

Of particular interest are the correlation functions which are the averages of products of occupation numbers or spin variables at different sites. The one-point correlation function $\langle \rho_n \rangle = [1 + \langle \sigma_n \rangle]/2$ is just the local concentration c_n which may depend on n in the presence of a site-dependent field h_n . From equations (5.40b) and (5.41) we have the identity

$$\langle \sigma_n \rangle = \frac{\partial \log \mathcal{Z}}{\partial \beta h_n}; \beta = 1/k_B T \quad (5.42)$$

Similarly the second derivatives of $\log \mathcal{Z}$ provide us with the two-point cumulant average

$$\langle \sigma_n \sigma_m \rangle_c = \langle \sigma_n \sigma_m \rangle - \langle \sigma_n \rangle \langle \sigma_m \rangle = \frac{\partial^2 \log \mathcal{Z}}{\partial \beta h_n \partial \beta h_m} \quad (5.43)$$

so that one-point and two-point averages are related through

$$X_{nm} = \frac{\partial \langle \sigma_n \rangle}{\partial h_m} = \langle \sigma_n \sigma_m \rangle_c / k_B T \quad (5.44)$$

When h_n is independent of n , $\langle \rho_n \rangle$ is in principle also independent of n and equal to the mean concentration c . However long range order (LRO) is precisely associated with a breaking of translational invariance and is therefore characterised by site-dependent concentrations or 'magnetisations'. Consider for example the B2(CsCl) ordered structure (Fig. 5.9) which can be divided into two simple cubic sublattices 1 and 2. A *long range order parameter* η can be defined from

$$\begin{aligned} \eta &= \langle \sigma_n \rangle & \text{if } n \text{ belongs to sublattice 1} \\ &= -\langle \sigma_n \rangle & \text{if } n \text{ belongs to sublattice 2} \end{aligned} \quad (5.45)$$

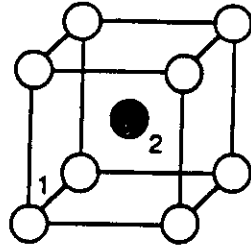


Fig. 5.9 B2 (CsCl structure).

More generally LRO parameters can be defined from any linear combinations of the deviations $\langle p_n \rangle - c$ or $\langle \sigma_n \rangle - m$. In this sense phase separation is also characterised by LRO parameters.

In the absence of long range order some local order is generally still present. Short range order (SRO) is usually characterised by the Warren–Cowley SRO parameters α_{nm}

$$\langle (p_n - c)(p_m - c) \rangle = c(1 - c)\alpha_{nm} \quad (5.46)$$

Comparing with equations (5.43) and (5.44), we have the relationship

$$X_{nm} = 4c(1 - c)\alpha_{nm} = (1 - m^2)\alpha_{nm} \quad (5.47)$$

By definition states such that $\alpha_{nm} = 0$ will be called *completely* disordered states, disordered states (or solid solutions) being characterised by vanishing LRO parameters. Strictly speaking completely disordered states only occur at infinite temperature.

5.7 ISING MODEL FOR ALLOYS AND ITS GROUND STATES

The Ising model is the simplest model describing interacting spins σ_n on a lattice

$$H(\{\sigma_n\}) = \frac{1}{2} \sum_{n,m} \mathcal{J}_{nm} \sigma_n \sigma_m - h \sum_n \sigma_n \quad (5.48)$$

In the alloy context this is just a model for the ordering energy involving pair interactions only (see, for example, the Appendix). If we drop any term independent of the configuration, it is straightforward to realise that \mathcal{J}_{nm} is precisely equal to the pair interaction $V_{nm}/4$ derived from the generalised perturbation expansion (see equation (5.28)). The second term on the r.h.s. of equation (5.48) is only relevant in the grand-canonical formulation and we recall that h plays the part of a chemical potential difference. The analogy between magnetic systems and alloys is frequently fruitful. One should keep in

mind that ordering in the usual sense for alloys corresponds to antiferromagnetic ordering whereas phase separation corresponds to ferromagnetic ordering.

The first problem we have to consider is to determine the ground state at zero temperature of the Ising model for various values of the interactions and of the field. The technique we are going to describe applies as well in fact to any generalized Ising model involving cluster interactions provided they are short-ranged. We then define cluster variables σ_α where α is a cluster, i.e. a set of lattice points $\{n_1, \dots, n_r\}$

$$\sigma_\alpha = \sigma_{n_1} \cdots \sigma_{n_r} \quad (5.49)$$

and a generalized Ising Hamiltonian

$$H(\{\sigma_n\}) = \sum_\alpha J_\alpha \sigma_\alpha \quad (5.50)$$

where here the interactions J_α are assumed to be independent of the concentration.

Assume we have found an ordered structure minimising the energy H . In general translational invariance is broken and different variants of the same structure have the same energy. Averaging over these variants restores this invariance. This is the limit at zero temperature of the thermodynamic average. The ground state energy E can therefore be written

$$E = \sum_\alpha J_\alpha \langle \sigma_\alpha \rangle \quad (5.51)$$

where in fact the correlation function $\langle \sigma_\alpha \rangle$ only depends on the type i (point, pair, triplet, . . .) of the cluster α . Let r_i be the number of such clusters in the lattice; E can then be written

$$E = \sum_i X_i x_i \quad (5.52)$$

with

$$X_i = r_i; x_i = \langle \sigma_i \rangle$$

E is a linear function of the x_i and is therefore minimum at the boundary of its domain of definition. The problem is then to derive appropriate constraints on the correlation functions. Obviously $|x_i| \leq 1$ but more inequalities are required. Consider an Ising model with first neighbour interactions. The relevant correlation functions are the point x_1 and pair x_2 correlation functions. Now, from the inequalities $\langle p_n p_m \rangle \geq 0$, $\langle p_n (1 - p_m) \rangle \geq 0$, $\langle (1 - p_n)(1 - p_m) \rangle \geq 0$, we deduce that

$$\begin{aligned} 1 \pm 2x_1 + x_2 &\geq 0 \\ 1 - x_2 &\geq 0 \end{aligned} \quad (5.53)$$

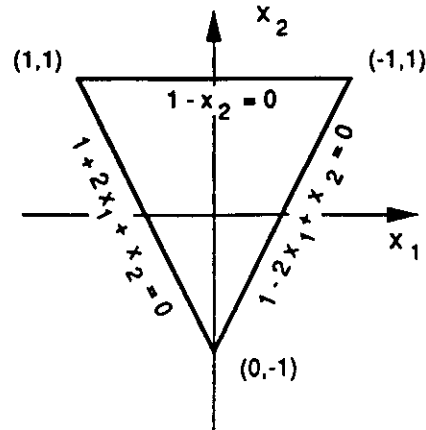


Fig. 5.10 Configurational triangle defined by the inequalities (7.6).

In the (x_1, x_2) plane this determines the interior of a triangle. On the other hand, for a fixed value of the energy, the equation $E = X_1 x_1 + X_2 x_2$ gives us the equation of a line normal to the vector (X_1, X_2) . Varying E , the line moves parallel to itself, so that its minimum is attained when the line passes through one of the vertices: the ground state corresponds to the vertices of the configurational triangle (Fig. 5.10). This is a familiar result of linear programming. The second step in the method is to look for the ordered structures associated with the vertices. There is no difficulty with the vertices $(1, 1)$ and $(-1, 1)$ which correspond to ferromagnetic ordering, i.e. to the pure elements in the alloy language. Consider now the third vertex $(0, -1)$. One then looks for antiferromagnetic ordering where all first neighbour pairs are of type $+ -$ (or AB in the alloy language). This is possible on some lattices: linear chain, simple cubic lattice, bcc lattice in which case the B2 structure is obtained, but not on other ones such as the triangular or the fcc lattice. Because of the presence of triangles in these structures, AA or BB pairs are unavoidable. This is a frustration effect which introduces new constraints. To determine them, we write that the numbers of BBB, BBA, BAA and AAA triangle configurations should be positive. These numbers are nothing but the averages $\langle p_a p_m p_p \rangle$, $\langle p_a p_m (1 - p_p) \rangle$, $\langle p_a (1 - p_m) (1 - p_p) \rangle$ and $\langle (1 - p_a) (1 - p_m) (1 - p_p) \rangle$ for a triangle nmp . Using spin variables and eliminating the triplet correlation function $\langle \sigma_n \sigma_m \sigma_p \rangle$, we obtain the three inequalities (equation (5.53)) plus the new inequality

$$1 + 3x_2 \geq 0 \quad (5.54)$$

The corresponding line cuts the configurational triangle and yields two new vertices which define ground states if it is possible to fill the lattice with triangles of type BBA or BAA (Fig. 5.11). This is clearly possible on a triangular lattice, but not on a fcc lattice. In the latter case inequalities corresponding to tetrahedron configurations should be introduced.

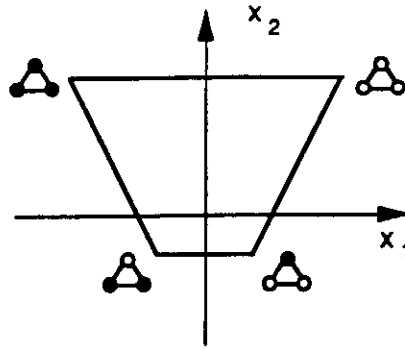


Fig. 5.11 Configurational polygon defined from the triangle inequalities. Each vertex is associated with a definite triangle configuration.

From the preceding examples, we can guess an adequate strategy. We must find various linear inequalities related to the geometry of the lattice under study and determine the corresponding configurational polyhedron in the space of correlation functions, using linear programming techniques when necessary. After that, we must inquire whether ordered structures can be associated with the vertices of this polyhedron. If this is the case the ground state is determined exactly. If not, new inequalities associated with larger clusters should be considered. These two last steps are difficult when many interactions are present; frustration effects then become very complex and there is no general rule to guess what are the clusters to consider in order to obtain the required inequalities. There is even no guarantee that these relevant clusters are necessarily of finite size. Counter-examples have been found. Anyway the algorithm is of exponential type since the number of configurations to study grows as $2^{|\alpha|}$ where $|\alpha|$ is the number of sites of the cluster α . Nevertheless its advantage is that in several cases of interest, in the case of short range interactions in particular, it can provide us with exact statements.

In practice the ground states in the presence of first and second neighbour interactions can generally be found exactly. It is then easy to determine the domains of stability (i.e. the phase diagrams) of the different ordered structures in the space of interactions. Many results in this field are due to Kanamori and co-workers. A complete discussion of this ground state analysis and many examples can be found elsewhere.¹ We just show here in Fig. 5.12 the domains of stability of the ordered structures on the fcc lattice with first and second neighbour interactions.

5.8 ORDER-DISORDER TRANSITION, MEAN FIELD AND LANDAU THEORIES

Although they are known to suffer from serious drawbacks when one is interested in a detailed analysis of critical phenomena, mean field theories still provide

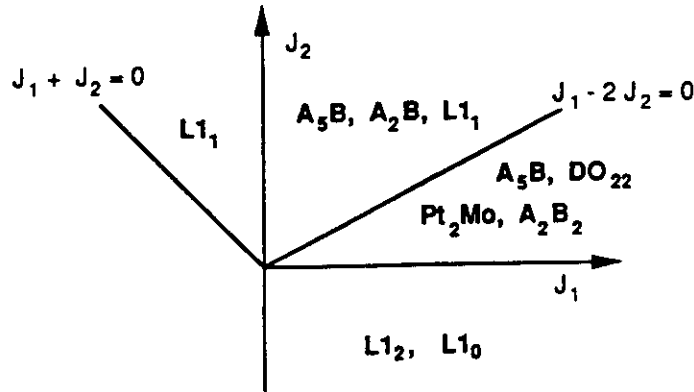


Fig. 5.12 Ground states of the fcc lattice with first and second neighbour interactions. Descriptions of the structures can be found in Ref. 1 or 18.

invaluable tools to investigate order-disorder phase transitions. Furthermore, modern generalised mean field methods such as the cluster variation method (CVM) are now known to be very accurate.

Mean field theories are always based on the following type of argument. Assume first that the atoms (or spins) are independent and only feel a field h_n at site n . The probability of having the configuration characterised by a set of σ_n , $\rho(\{\sigma_n\})$ is given by (see equation (5.41b))

$$\rho(\{\sigma_n\}) = \frac{1}{Z} \exp \left[\sum_n \beta h_n \sigma_n \right] \quad (5.55)$$

Taking the trace over all spin variables except σ_n we obtain the probability $\rho_n(\sigma_n)$ of having the spin σ_n at site n . It should therefore be proportional to $\exp(\beta h_n \sigma_n)$. Since $\text{Tr} \rho_n = 1$ by definition, we obtain

$$\rho(\sigma_n) = \frac{\exp(\beta h_n \sigma_n)}{2 \cosh \beta h_n} \quad (5.56a)$$

so that

$$\langle \sigma_n \rangle = \text{Tr} \rho_n \sigma_n = \tanh \beta h_n \quad (5.56b)$$

In the presence of interactions, it is no longer possible to calculate $\rho(\sigma_n)$ exactly but we shall assume that the behaviour of a definite spin only depends on the average values of the other ones. This amounts to replacing h_n by an effective or mean field h_n^{eff}

$$h_n^{\text{eff}} = h_n - \sum_m J_{nm} \langle \sigma_m \rangle \quad (5.57)$$

Hence the self-consistent mean field (or Bragg-Williams-Gorski) equations for $\langle \sigma_n \rangle$

$$\langle \sigma_n \rangle = \tanh \beta h_n^{\text{eff}} = \tanh \beta \left(h_n - \sum_m \mathcal{J}_{nm} \langle \sigma_m \rangle \right) \quad (5.58a)$$

Using the concentrations instead of the magnetisations, this may also be written

$$\frac{c_n}{1 - c_n} = \exp \beta h_n^{\text{eff}} \quad (5.58b)$$

Another standard derivation uses the variational properties of the free energy. If short range order is neglected, $\langle \sigma_n \sigma_m \rangle$ is replaced by $\langle \sigma_n \rangle \langle \sigma_m \rangle$ and the internal energy is approximated by $\frac{1}{2} \sum_{n,m} \mathcal{J}_{nm} \langle \sigma_n \rangle \langle \sigma_m \rangle$. Adding the entropy term of independent atoms, we obtain the free energy $\hat{F}(\{\langle \sigma_n \rangle\})$

$$\begin{aligned} \hat{F}(\{\langle \sigma_n \rangle\}) &= \frac{1}{2} \sum_{n,m} \mathcal{J}_{nm} \langle \sigma_n \rangle \langle \sigma_m \rangle - \sum_n h_n \langle \sigma_n \rangle \\ &+ k_B T \left\{ \frac{1 + \langle \sigma_n \rangle}{2} \log \frac{1 + \langle \sigma_n \rangle}{2} + \frac{1 - \langle \sigma_n \rangle}{2} \log \frac{1 - \langle \sigma_n \rangle}{2} \right\} \end{aligned} \quad (5.59)$$

and one can check that the mean field equations are recovered when we impose $\partial \hat{F}(\{\langle \sigma_n \rangle\}) / \partial \langle \sigma_n \rangle = 0$ for any n . This formulation has the advantage of providing us with an approximation for the free energy and not only for the point correlation functions.

Let us recall the familiar application of these equations to B2 ordering on a bcc lattice (Fig. 5.9) in the case of first neighbour interactions \mathcal{J} . At stoichiometry, $c = 1/2$ and therefore $h = 0$. Using equation (5.45) we obtain

$$\eta = \tanh 8\beta \mathcal{J} \eta \quad (5.60)$$

When $k_B T < 8\mathcal{J}$ there are three solutions (Fig. 5.13), but the disordered solution $\eta = 0$ has a larger free energy than the two other symmetric ones: the ordered solutions are stable, and translational symmetry is spontaneously broken. In this case the LRO parameter η vanishes continuously at the critical temperature according to a square root law $\eta \approx (T_c - T)^{1/2}$ with $k_B T_c = 8\mathcal{J}$ (Fig. 5.14a). The order-disorder transition is said to be *continuous* or *of second order*. In other cases, such as when considering L1₂ ordering (see below), the transition is *discontinuous* or *of first order* (Fig. 5.14b).

The cluster variation method (CVM) put forward by Kikuchi in the fifties is a natural extension of the previous single site mean field theory, the idea being to treat clusters (instead of single sites) embedded in an average medium.

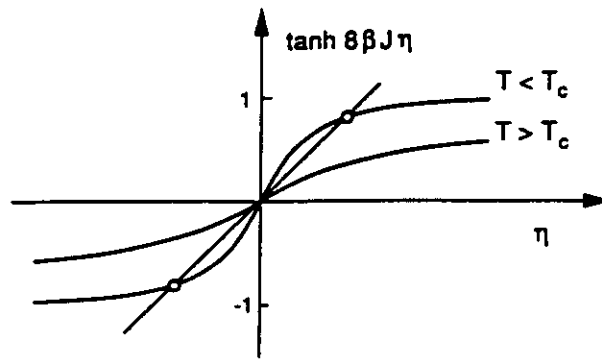


Fig. 5.13 Graphical solution of the equation $\eta = \tanh 8\beta J \eta$.

The major improvement brought by this method concerns the configurational entropy which is very badly treated in the usual mean field approximation (MFA), since correlations between the occupations of different sites are completely neglected. As a result the critical temperatures determined within the MFA are generally much too high, particularly when frustration effects are important. There are some difficulties in determining the most appropriate clusters and also in handling them when they are large, but the method is now well developed and reproduces the 'exact' critical temperature as determined from Monte Carlo simulations or series expansions with a very good accuracy. Several reviews on the CVM are now available.^{1,18-22}

Many features of the order-disorder transitions can be understood using Landau phenomenological theory. This theory is based on a general qualitative study of the mean field free energy functional and of their symmetry properties. We apply it here to a discussion of the functional $\hat{F}(\{\langle \sigma_n \rangle\})$. Let us use alloy variables and define the concentration fluctuations $\delta c_n = c_n - c$. We now compare the corresponding canonical free energy with that of the disordered

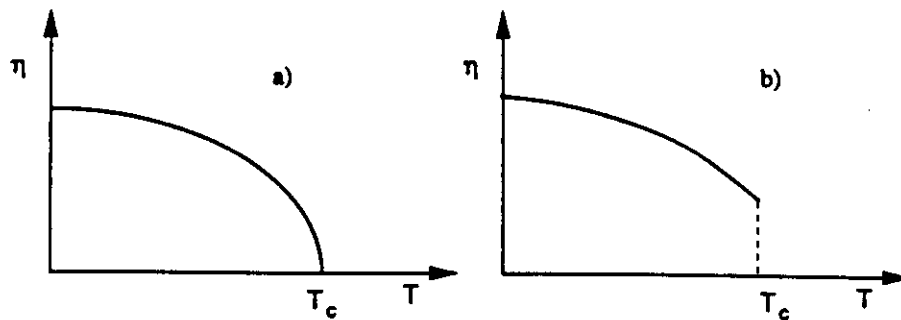


Fig. 5.14 Variations of the order parameter as a function of temperature, (a) for second order transitions; (b) for first order transitions.

state

$$\delta\hat{F}(c, \{\delta c_n\}) = \hat{F}(c, \{\delta c_n\}) - \hat{F}(c, \{\delta c_n = 0\}) \quad (5.61)$$

with

$$\begin{aligned} \hat{F}(c, \{\delta c_n\}) &= \frac{1}{2} \sum_{n,m} V_{nm} c_n c_m \\ &\quad + k_B T \sum_n \{c_n \log c_n + (1 - c_n) \log (1 - c_n)\} \end{aligned}$$

We recall that $V_{nm} = 4\mathcal{J}_{nm}$. Expanding $\delta\hat{F}(c, \{\delta c_n\})$ in powers of δc_n , we obtain

$$\begin{aligned} \delta\hat{F}(c, \{\delta c_n\}) &= \frac{1}{2} \sum_{n,m} \left(V_{nm} + \frac{k_B T}{c(1-c)} \delta_{nm} \right) \delta c_n \delta c_m \\ &\quad + k_B T \frac{2c-1}{6} \sum_n (\delta c_n)^3 + \dots \end{aligned} \quad (5.62)$$

Using then Fourier transforms of δc_n and of $V_{nm} = V(m-n)$

$$\delta c_n = \sum_k e^{ik \cdot n} \delta c_k; \quad V(k) = \sum_R e^{ik \cdot R} V(R) \quad (5.63)$$

we obtain

$$\begin{aligned} \delta\hat{F}(c, \{\delta c_k\}) &= \frac{1}{2} \sum_k \left(V(k) + \frac{k_B T}{c(1-c)} \right) |\delta c_k|^2 \\ &\quad + k_B T \frac{2c-1}{6} \sum'_{k_1, k_2, k_3} \delta c_{k_1} \delta c_{k_2} \delta c_{k_3} + \dots \end{aligned} \quad (5.64)$$

where the prime in the sum means that $k_1 + k_2 + k_3$ should be equal to a reciprocal vector of the underlying lattice.

The coefficient of the quadratic part of $\delta\hat{F}$ is positive at high temperature and then the disordered phase characterised by $\delta c_k = 0$ is stable. When the temperature decreases, it becomes unstable at a critical temperature $T_c(k_0)$ for the concentration fluctuations of wave vector k_0 such that

$$k_B T_c(k_0) = -c(1-c)V(k_0) \quad (5.65)$$

Consider again the BCC lattice with positive first neighbour interactions $\mathcal{J} = V/4$ and when $c = 1/2$. The most unstable concentration wave is then

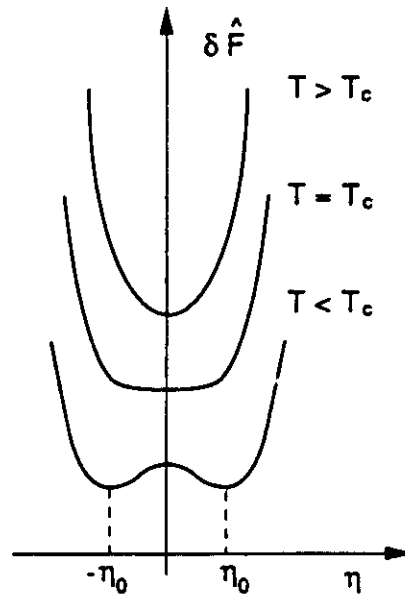


Fig. 5.15 Free energy as a function of the order parameter η for a second order transition. η_0 and $-\eta_0$ are the equilibrium values of η below T_c .

[100] in units of $2\pi/a$, where a is the lattice parameter and we recover the critical temperature $k_B T_c = 8\mathcal{J}$. Notice here that the wave [010] and [001] are strictly equivalent to [100] in the sense that they differ from a vector of the reciprocal lattice of the bcc lattice. Up to a normalisation factor we see that the order parameter η is nothing but the amplitude of the concentration waves which allows us to describe the B2 ordered structure.^{1,18,23} In the present case there is a single wave to consider and the order parameter is scalar. Keeping only this wave in the free energy we obtain an expansion of the form

$$\delta F(\eta) = \frac{1}{2}t\eta^2 + u\eta^4 + \dots \quad (5.66)$$

where odd powers of η are absent since changing η into $-\eta$ amounts to replacing one variant of the B2 structure by the other. Hence the familiar behaviour of the free energy as a function of the temperature (Fig. 5.15).

In the fcc lattice and at stoichiometry A_3B , positive first neighbour interactions favour ordering according to the $L1_2$ (Cu_3Au) structure (Fig. 5.18), (in fact other interactions are necessary to lift the degeneracy of this structure with other ones).¹ To describe this structure we need the three waves [100], [010] and [001] with a common amplitude η ; actually in the fcc lattice they are not equivalent modulo a vector of the reciprocal lattice. On the other hand the sum of these wave vectors is equal to such a vector, which means that cubic terms in the Landau expansion no longer vanish. Using standard arguments this proves that the $L1_2$ order-disorder transition should be of first order and occurs

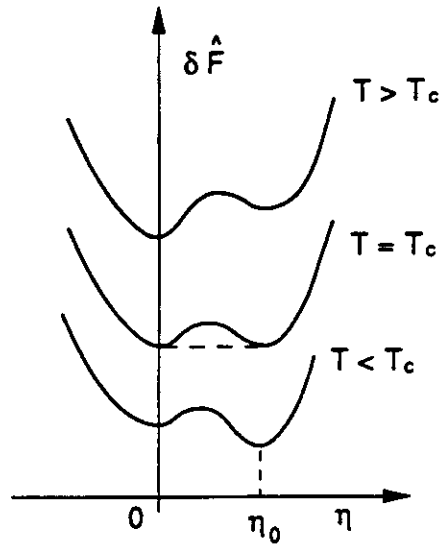


Fig. 5.16 Free energy for a first order transition.

above the temperature $T_c(k_0)$. Figure 5.16 shows the corresponding behaviour of the free energy

$$\delta \hat{F}(\eta) = \frac{1}{2} r \eta^2 + w \eta^3 + u \eta^4 + \dots \quad (5.67)$$

Notice that the presence of three waves indicates that the order parameter in this case should be considered as a vector with three components. This is important when studying for example interfaces between different variants of $L1_2$.^{24,25}

Landau theory therefore allows us to make predictions concerning the nature of the ordered phases and of the order of the transitions. This is described in detail elsewhere.^{1,18,23}

We now consider short-range order. In principle the simplest mean field theory neglects it but some information can be recovered by using equation (5.44) which relates $\langle \sigma_n \sigma_m \rangle_c$ to the derivative $\partial \langle \sigma_n \rangle / \partial h_m$. Using the MFA equations in the presence of inhomogeneous external fields h_n we can obtain a closed formula for the Fourier transform $\alpha(k)$ of the SRO parameters α_m which only depend on $m-n$ in the disordered phase. This is the so-called Krivoglaz-Clapp-Moss (KCM) formula

$$\alpha(k) = [1 + c(1 - c)V(k)/k_B T]^{-1} \quad (5.68)$$

This is obviously not a consistent treatment of SRO since, for instance, $\alpha(k_0)$ diverges at the critical temperature $T_c(k_0)$ whereas the initial MFA approximation corresponds to set $\alpha(k) = 1$. However the KCM formula is exact to order

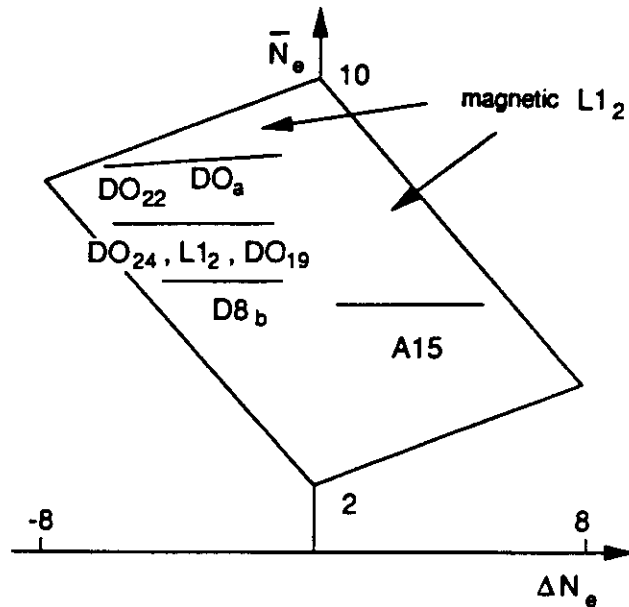


Fig. 5.17 Schematic structure map for A_3B compounds.

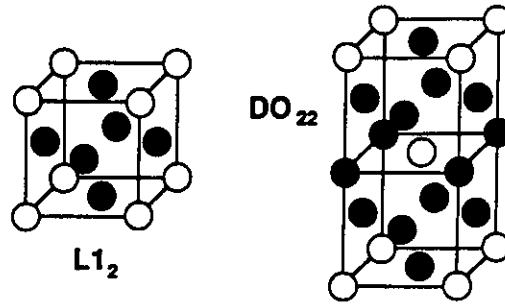
$1/T$ at high temperature and provides us with a reasonable first approximation. The fact that $\alpha(k)^{-1}$ is proportional to the coefficient of the quadratic part of the Landau free energy functional is not fortuitous at all since both quantities measure the response of the disordered state to concentration fluctuations in a harmonic analysis. Similar although more complicated formulae can be derived within the CVM.

5.9 APPLICATIONS

All the ingredients to understand the behaviour of specific systems are now available. We discuss some applications which will hopefully give a flavour of the present state of the art.

5.9.1 ORDERED STRUCTURES OF TRANSITION ALLOYS

Transition alloys are well described qualitatively within the tight-binding scheme presented in the first part of this chapter. We recall that the important alloy parameters are the alloy parameter δ/\bar{W} and the filling of the band \bar{N}_e . Since δ is itself approximately proportional to $\Delta N_e = N_e^B - N_e^A$, it is quite natural to classify the structures by using the coordinates ΔN_e and \bar{N}_e .²⁶ Such maps are very successful in that the different ordered structures generally belong to different non-overlapping domains. We comment here on the map at $c = 1/4$ (Fig. 5.17); other maps are discussed in Refs. 1, 26 and 27. Lists of

Fig. 5.18 L1₂ and DO₂₂ structures.

structures are available in Refs. 26 and 27. We shall consider here just the simplest ones. At $c = 1/4$ we keep the familiar L1₂ and DO₂₂ structures built on the fcc lattice (Fig. 5.18) as well as the equivalent structures on the hcp (DO₁₉ and DO₃) or double hcp lattice (DO₂₄), and the A15 structure.

The ordering tendencies are quite clear. A15 appears when $\Delta N_i > 0$ and all other non-magnetic structures when $\Delta N_i < 0$. Note that our sign convention is such that for instance ΔN_i is positive for PtV₃ but negative for Pt₃V (we always assume a compound A₃B). It is also striking that all DO₂₂ structures, plus the 'equivalent' DO₃ structure occur at the same point, $\bar{N}_i = 7.75$, $\Delta N_i = -5$ and therefore correspond to elements of the column of vanadium and of that of nickel. The non-magnetic L1₂ structures are all in the range $6.5 \leq \bar{N}_i \leq 7.5$ whereas most equivalent hexagonal structures occur for $\bar{N}_i = 7.25$.

From the theoretical side, consider first the fcc lattice. We know that in general $|V_1| \gg |V_2, V_3, V_4| \gg |V_5, V_6, \dots|$, so that ordered structures only appear when $V_1 > 0$. Calculating V_1 from the electronic structure defines a domain in which non-magnetic systems may order. Now, on the fcc lattice and for $c = 1/4$, the only possible ground states in the presence of interactions up to fourth neighbours are L1₂ and DO₂₂. The two structures have identical numbers of AB first neighbour pairs, which means that the difference in energy between them is much smaller than V_1 . It is given by the combination $\xi = V_2 - 4V_3 + 4V_4$, and moment arguments show that ξ should have at least four zeros as a function of band filling. Tight-binding calculations then clearly show a stability exchange between L1₂ and DO₂₂ for \bar{N}_i about seven, in good agreement with the observed structures (Fig. 5.19). Large values of \bar{N}_i are irrelevant (since there is no order) as well as small ones (since the lattice is no longer fcc). These results have been confirmed by more sophisticated electronic structure calculations.

The stability of DO₂₂ for large electron numbers is therefore explained. If we now compare different crystalline structures, the GPM is of no direct use and full calculations should be undertaken although there is some hope that structural energies can also be analysed in terms of pair and multi-atom interactions.

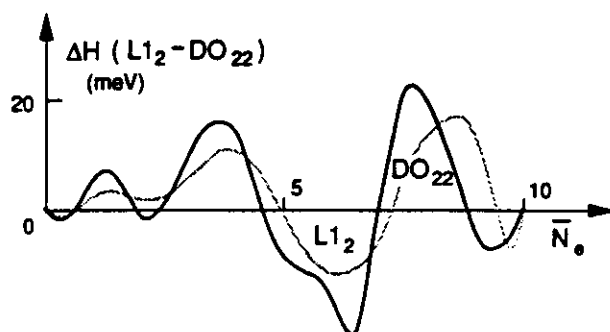


Fig. 5.19 Calculated energy difference between $L1_2$ and DO_{22} as a function of the number of d electrons.⁷ Continuous line: full calculation; dotted line: calculation with pair interactions up to V_4 .

Simple arguments tell us on the other hand that BCC or more complex structures should be favoured when $\bar{N}_d \approx 5-6$ and it is therefore not surprising that A15 is the most stable structure here.

Such simple arguments inherited from the study of elemental metals do not apply in the case of the cubic-hexagonal competition when $\Delta\bar{N}_d < 0$. Actually both the fcc-hcp and the $L1_2$ - DO_{22} energy differences are very small and the interplay between chemical and structural effects has still to be investigated in detail.

There are numerous other examples showing that simple theoretical arguments predict the correct structural trends. For example the hierarchy between the interactions on a fcc lattice shows that it is generally necessary to include third and fourth neighbour interactions as soon as second neighbour interactions are introduced. This is frequently verified, in the case of transition alloys at least. Actually many observed ordered structures require at least fourth neighbour interactions to be stabilised. Conversely a structure like that of $\text{CuPt}(L1_1)$ requires second neighbour interactions comparable with the first neighbour ones and is in fact never observed except precisely in the case of CuPt !

Other hierarchies are expected in different types of compounds. The case of substoichiometric NaCl transition carbides and nitrides is very instructive in this respect. Here ordering of vacancies takes place in the fcc sublattice occupied by interstitial (carbon or nitrogen) atoms but these atoms principally interact with the metallic atoms of the other sublattice. A simple moment analysis shows that we should then have the hierarchy $|V_2| > |V_1| \gg \dots$, which favours structures very different from those met in transition alloys. In particular the CuPt -type structure is found to be very stable, which is actually observed.^{29,30} Pseudobinary semiconductor alloys form another category of compounds which has been studied in detail.³¹

As another example illustrating how we have elucidated trends, consider the nickel based transition alloys, in particular their phase diagrams as compiled

by de Boer *et al.*⁵ When ΔN_i is small, ordering is absent except in Pt-Ni. Small values of ΔN_i imply small almost unobservable transition temperatures, and anyway large values of \bar{N}_i induce a tendency to phase separation. For the case of 4d and 5d alloying elements, except for Pt-Ni, there is indeed no ordering tendency up to Tc and Re. Ordering effects in Ni-Fe and Ni-Mn are clearly correlated with the appearance of magnetism (an extensive discussion of the interplay between magnetic and chemical ordering has been given recently by Bieber and Gautier³²). Weak ordering effects appear when ΔN_i increases. Ni-Mo and Ni-W present ordered phases whereas SRO effects have clearly been detected in Ni-Cr. This is consistent with the fact that the order of magnitude of ordering energies should increase with the bandwidth, i.e. when going from the 3d to the 5d series. The same phenomenon exists for the vanadium column: on the Ni-rich side of the diagrams there are ordered structures on the fcc lattice which disorder at high temperature in the case of Ni-V but not in the case of Ni-Nb and Ni-Ta. Finally many very stable ordered compounds appear when ΔN_i is equal to 6 and 7. Thus, except for the ordering in Pt-Ni which is still a subject of controversy, almost all is understood qualitatively for the case of Ni based alloys. This is certainly a somewhat favourable situation, but many other successful analyses have been made. For example, the fact that off-diagonal disorder induces phase separation is well verified in the case of Cr-Mo and Cr-W alloys.

If one is interested in a particular system rather than in trends, then first principles calculations of total energies are obviously preferable if they are accurate enough, which now begins to be the case. By performing several such calculations it is also possible to determine through an inverse procedure the interactions of an effective Ising model.³³ An advantage of the first principles methods is that they can handle non-transition elements as well. Aluminium based alloys, in particular, have been considered in some detail.

5.9.2 DIFFUSE SCATTERING AND SHORT RANGE ORDER

Diffuse X-ray or neutron scattering is a very efficient tool to measure short-range order effects. In fact, provided that other contributions due to atomic displacements or to magnetic effects are separated out, the diffuse intensity is proportional to $\alpha(k)$, the Fourier transform of the SRO parameter. If the Krivoglaz-Clapp-Moss formula (equation (5.6.8)) is valid, this yields the Fourier transform of the pair interactions $V(k)$. For a given set of interactions it is then possible to relate $\alpha(k)$, measured in the high temperature disordered phase, to the observed ground states at low temperature.

For example, assuming interactions up to the fourth neighbours in the fcc lattice, it is known that the stable ordered structures at the A_3B stoichiometry are $L1_2$ or DO_{22} depending on the sign (negative or positive, respectively) of the quantity $\zeta = V_2 - 4V_3 + 4V_4$, provided that V_1 is positive and sufficiently large. The KCM formula then predicts that $\alpha(k)$ is maximum for wave vectors

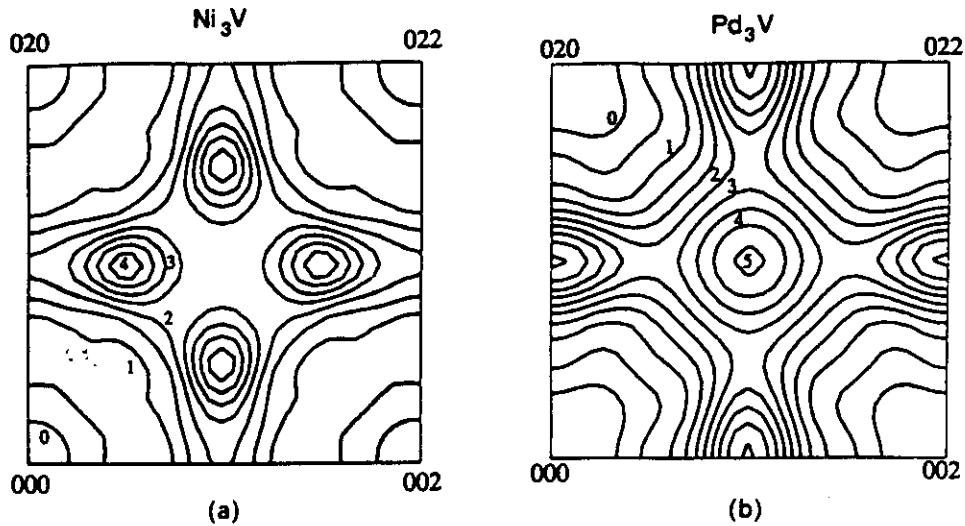


Fig. 5.20 Diffuse intensity in the (110) reciprocal plane obtained from neutron scattering (Laue units): (a) for Ni_3V ; (b) for Pd_3V .³⁸

of type (100) for L1_2 and $(1\frac{1}{2}0)$ for DO_{22} . This is observed in many systems, for example in Ni_3V which is DO_{22} at low temperature (Fig. 5.20a). Surprisingly enough measurements on Pd_3V which also orders according to DO_{22} show maxima at positions (100) (Fig. 5.20b). This breakdown of the usual mean field theory has been successfully explained using more accurate CVM approximations. It turns out that if ξ/V_1 is positive but small enough, the short range order above DO_{22} should actually be of the L1_2 type.³⁴ Experiment thus tells us that $\xi \approx 0$ in Pd_3V . Qualitative electron microscopy studies indicate that the situation is the same for Pt_3V . Using the structure maps, one can then predict that alloys with a slightly lower number of d electrons should order according to L1_2 . This has been recently verified by considering pseudobinary alloys $(\text{PtRh})_3\text{V}$ and $(\text{PtRh})_3\text{V}$ alloys.³⁵

Diffuse scattering experiments are now fairly accurate. Combined with appropriate CVM or Monte Carlo analyses they now provide us with reliable estimates of the pair interactions. Recent results concerning Cu-Zn, Au-Ag and Ni based alloys are given and discussed in Refs. 36 to 38.

5.9.3 PHASE DIAGRAMS

It is more difficult to calculate phase diagrams than to characterise the single phases, one reason being that it is not sufficient to know the interatomic chemical interactions. The free energy of the disordered state is also required. Although it can be calculated in principle, using the CPA for example, additional contributions related to elastic, vibrational and other effects have to be included. Another serious difficulty is that real phase diagrams frequently

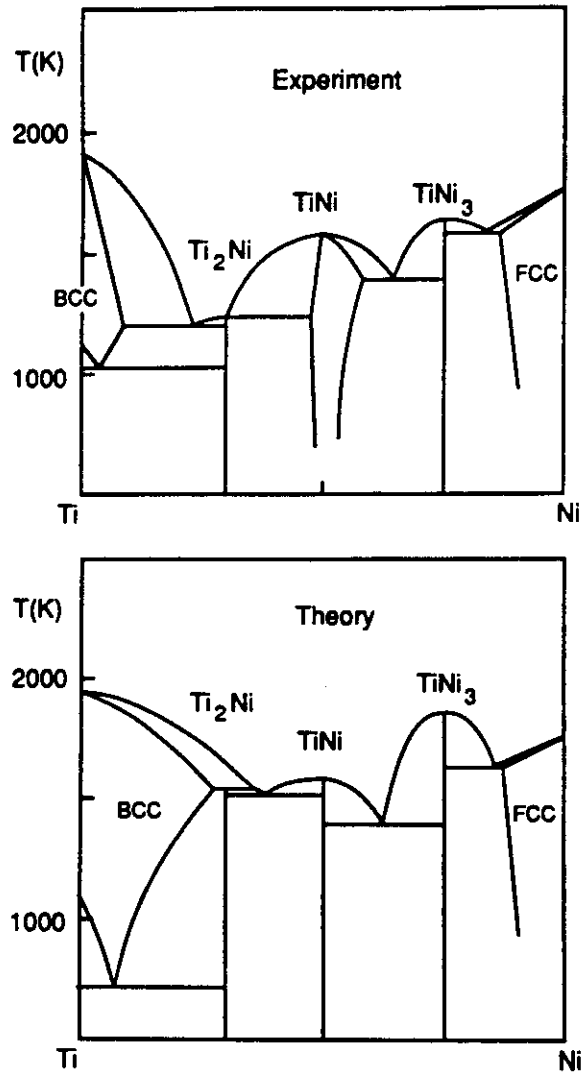


Fig. 5.21 Experimental and calculated phase diagram of Ti-Ni.⁴⁵

involve different crystalline structures, and at the moment there is no elaborate theory to describe the interplay between structural and chemical (ordering) effects. In practice, ordering effects are treated on fixed lattices and the free energies for different structures are compared. This is a correct procedure but the uncertainties concerning the structural energies or entropies are difficult to estimate, and generally some parameters have to be fitted to experimental data in order to produce reasonable phase diagrams. It is clear also that it is difficult to treat the liquid state on the same footing as the solid phases.

Despite all these problems several phase diagrams have now been calculated.

There is no room here to undertake a comprehensive review of these results. We just mention some calculations concerning the Ti-Rh,³⁹ Ni-Cr,⁴⁰ Pd-Rh, and Al-Li⁴¹ phase diagrams and the recent detailed discussions concerning the Ni-Ti and Ni-Al phase diagrams.^{42,43} The experimental and calculated diagrams of Ti-Ni are shown in Fig. 5.21.

REFERENCES

1. F. Ducastelle, *Order and Phase Stability in Alloys, Cohesion and Structure*, Vol. 3, (ed. F.R. de Boer and D.G. Pettifor), North-Holland, Amsterdam, 1991.
2. D. de Fontaine, *Solid State Phys.*, 1979, **34**, 73.
3. J. Hafner, *From Hamiltonians to Phase Diagrams*, Springer, Berlin, 1987.
4. A.G. Khachatryan, *The Theory of Structural Transformations in Solids*, Wiley & Sons, New York, 1983.
5. F.R. de Boer, R. Boom, W.C.M. Matens, A.R. Miedema and A.K. Niessen, *Cohesion in metals: Transition Metals Alloys, Cohesion and Structure*, Vol. 1, (ed. F.R. de Boer and D.G. Pettifor), North-Holland, Amsterdam, 1989; J. Hafner, F. Hulliger, W.B. Jensen, J.A. Majewski, K. Mathis, P. Villars and P. Vogl, *Cohesion in metals: Transition Metals Alloys, Cohesion and Structure*, Vol. 2 (ed. F.R. de Boer and D.G. Pettifor), North-Holland, Amsterdam, 1989.
6. F. Ducastelle, Electronic Structure, Effective Pair Interactions and Order in Alloys, in *Alloy Phase Stability*, (ed. G.M. Stocks and A. Gonis), NATO-ASI Series E, Vol. 163, Kluwer, Dordrecht, 1989.
7. A. Bieber, F. Ducastelle, F. Gautier, G. Treglia and P. Turchi, *Solid State Communications*, 1983, **45**, 585.
8. M. Sluiter and P.E.A. Turchi, *Phys. Rev.*, 1989, **B40**, 11 215.
9. L.G. Ferreira, S.H. Wei and A. Zunger, *Phys. Rev.*, 1989, **B40**, 3197.
10. S.H. Wei, L.G. Ferreira and A. Zunger, *Phys. Rev.*, 1990, **B41**, 8240.
11. A. Gonis, X.G. Zhang, A.J. Freeman, P. Turchi, G.M. Stocks and D.M. Nicholson, *Phys. Rev.*, 1987, **B36**, 4630.
12. H. Dreysse, A. Berera, L.T. Wille and D. de Fontaine, *Phys. Rev.*, 1989, **B39**, 2242.
13. M. Asta, C. Wolverton, D. de Fontaine and H. Dreysse, *Phys. Rev.*, 1991, **B44**, 4907; C. Wolverton, M. Asta, H. Dreysse and D. de Fontaine, *Phys. Rev.*, 1991, **B44**, 4914.
14. P.E.A. Turchi, G.M. Stocks, W.H. Butler, D.M. Nicholson and A. Gonis, *Phys. Rev.*, 1988, **B37**, 5982; P.E.A. Turchi, M. Sluiter, F.J. Pinski, D. Johnson, D.M. Nicholson, G.M. Stocks and J.B. Staunton, *Phys. Rev. Lett.*, 1991, **67**, 1779.
15. A. Bieber, *Thèse de Doctorat d'Etat, Université Louis Pasteur, Strasbourg*, 1987.
16. A. Bieber and F. Gautier, *J. Phys. Soc. Japan*, 1984, **53**, 2061 and *Zeitschrift für Physik*, 1984, **B57**, 335.
17. See e.g. P. Haasen, *Phys. Metall*, Cambridge University Press, Cambridge, 1978.
18. D. de Fontaine, *Solid State Phys.*, 1979, **34**, 73.
19. D. Gratias, 'Introduction aux Méthodes de Champ Moyen: la Méthode Variationnelle des Amas, in *L'Ordre et le Désordre dans les Matériaux*, Les Editions de Physique, Les Ulis, 1984, p. 119.
20. J.M. Sanchez, F. Ducastelle and D. Gratias, *Physica*, 1984, **128A**, 334.
21. D. de Fontaine, 'The Cluster Variation Method and the Calculation of Alloy Phase Diagrams, in *Alloy Phase Stability*, (ed. G.M. Stocks and A. Gonis), NATO-ASI Series E, Vol. 163, Kluwer, Dordrecht, 1989.

22. A. Finel, *Thèse de Doctorat d'Etat, Université Paris VI*, 1987.
23. A.G. Khachaturyan, *Progress in Mater. Sci.*, 1978, **22**, 1, and *The Theory of Structural Transformations in Solids*, Wiley, New York, 1983.
24. F. Ducastelle, Thermodynamics of surfaces and interfaces, in *Structural and Phase Stability of Alloys* (ed. J.L. Morán-López, F. Mejía-Lira and J.N. Sanchez), Plenum Press, New York and London, 1992.
25. A. Finel, V. Mazauric and F. Ducastelle, *Phys. Rev. Lett.*, 1990, **65**, 1016.
26. A. Bieber and F. Gautier, *Acta Metall.*, 1986, **34**, 2291.
27. M. Sluiter, P. Turchi and D. de Fontaine, *J. Physics F: Met. Phys.*, 1987, **17**, 2163.
28. S. Pei, T.B. Massalski, W.M. Temmerman, P.A. Sterne and G.M. Stocks, *Phys. Rev.*, 1989, **B39**, 5767.
29. J.P. Landesman, G. Tréglia, P. Turchi and F. Ducastelle, *Journal de Physique*, 1983, **46**, 1001; D.H. Le, C. Colinet and A. Pasturel, *Physica B*, 1991, **168**, 285.
30. C.H. De Novion and J.P. Landesman, *Pure and Applied Chem.*, 1985, **57**, 1391; *Nonstoichiometric Compounds; Advances in Ceramics*, Vol. 23, The American Ceramic Society, 1987.
31. S.H. Wei, L.G. Ferreira and A. Zunger, *Phys. Rev.*, 1990, **B41**, 8240.
32. A. Bieber and F. Gautier, *J. Magnetism and Magnetic Mater.*, 1991, **99**, 293.
33. Z.W. Lu, S.H. Wei, A. Zunger, S. Frota-Pessoa and L.G. Ferreira, *Phys. Rev.*, 1991, **B44**, 512, and references therein.
34. F. Solal, R. Caudron, F. Ducastelle, A. Finel and A. Loiseau, *Phys. Rev. Lett.*, 1987, **58**, 2245.
35. E. Cabet and A. Loiseau, private communications and to be published.
36. L. Reinhard, B. Schönfeld, G. Kostorz and W. Bührer, *Phys. Rev.*, 1990, **B41**, 1727; P.E.A. Turchi, M. Sluiter, F.J. Pinski, D.D. Johnson, D.M. Nicholson, G.M. Stocks and J.B. Staunton, *Phys. Rev. Lett.*, 1991, **67**, 1779.
37. B. Schönfeld, J. Traube and G. Kostorz, *Phys. Rev.*, 1992, **B45**, 613.
38. R. Caudron, M. Sarfati, M. Barrachin, A. Finel, F. Ducastelle and F. Solal, to be published in *Journal de Physique*, 1992.
39. M. Sluiter, P. Turchi, F. Zezhong and D. de Fontaine, *Phys. Rev. Lett.*, 1988, **60**, 716.
40. N.C. Tso, M. Kosugi and J.M. Sanchez, *Acta Metall.*, 1989, **37**, 121.
41. D.D. Johnson, P.E.A. Turchi, M. Sluiter, D.M. Nicholson, F.J. Pinski and G.M. Stocks, *Mater. Res. Soc. Symp. Proc.*, 1991, **186**, 21; A. Gonis, P.E.A. Turchi, M. Sluiter, F.J. Pinski and D.D. Johnson, *Mater. Res. Soc. Symp. Proc.*, 1991, **186**, 89.
42. D.H. Le, C. Colinet, P. Hicter and A. Pasturel, *J. Phys: Condensed Matter*, 1991, **3**, 7895 and 9965.
43. A. Pasturel, C. Colinet, A.T. Paxton and M. Van Schilfgaarde, *J. Phys: Condensed Matter*, 1992, **4**, 945; C. Colinet, P. Hicter and A. Pasturel, *Phys. Rev.*, **B45**, 1571; see also M. Sluiter, P.E.A. Turchi, F.J. Pinski and G.M. Stocks, to be published in *J. Phase Equilibria*.

